SEISMIC PERFORMANCE OF A 3D PRECAST/POST-TENSIONED REINFORCED CONCRETE SUB-STRUCTURE UNDER BI-AXIAL LOADS

C.T. Cheng[1], H.H. Chen[2], K.C. Lin[3], P. C Chen[4] and S.J. Jhuang[4]

[1] *Associate Professor, Department of Construction Engineering, Kaohsiung First University of Science & Technology, Kaohsiung, Chinese Taiwan*
Email: ctcheng@ccms.nkfust.edu.tw
[2] *Graduate Student, Kaohsiung First University of Science and Technology*
[3] *Associate Research Fellow, Center for Research on Earthquake Engineering (NCREE), Chinese Taiwan*
[4] *Assistant Research Fellow, Center for Research on Earthquake Engineering (NCREE), Chinese Taiwan*

ABSTRACT :

The precast and post-tensioned structures can be designed to have self-centering function that minimizes permanent drift after an earthquake. The self-centering function is achieved through the post-tensioned strands in the precast beams that allow the gap-open in the beam-column interface during earthquakes. Literatures have proved that the self-centering was effective for the beam-column connections. In real structure, there are floors that usually designed as a rigid diaphragm to transfer the seismic loads between gravity and moment-resisting frames; it may limit the gap-open in the beam-column interface of the self-centering structures. Therefore, a new design of the floor system that also has self-centering features is proposed. In order to investigate the self-centering function in real structure, a one-story 3D precast and post-tensioned sub-structure was constructed and tested. The tested specimen consists of four columns, four beams and one slab, representing one gravity frame, one moment resisting frame and the floor system that connects both frames. This test aims to investigate the force transfer by the floor slab as well as the seismic performance of the structure, in which the gaps in the beam-column and beam-floor interfaces may be opened in two directions, when subjected to bi-axial lateral loads. The investigated parameters include the prestress applied in the transfer beams that connected gravity and post-tensioned frames, installation of the energy dissipating steel angles in the post-tensioned frame and loading compositions.

KEYWORDS: full-scale testing, precast concrete, post-tensioned, self-centering, seismic performance, bi-axial loads

1. INTORDUCTION

In 2003 Christopoulos et al. and Ricles et al. investigated the self-centering function of beam-column connections after earthquake loads. They proved that the self-centering could effectively minimize residual drift after seismic loads in the prestressed beam-column connections. Under extreme loads, the self-centering function is achieved by the gap-open in the beam to column interface that eliminates the plastic deformation at the beam-ends. And then the prestress inside the beams forces the structure returning to its original position after loads. However, in real structures, the role of the floor in the self-centering structure is not clarified yet. If the floor slab is designed to be a rigid diaphragm integrating beams and columns together like the conventional structures, this floor slab may constrain the gap-open in the self-centering connections. As a result, Garlock and Li 2005 proposed a new floor detail using collector beams to transfer the seismic loads between frames, but required it soft enough not to hinder the gap-open in the connections at the same time. Cheng and Ke 2007 proposed a new concept for the design of floor slab in the self-centering structure by using precast/post-tensioned slab. The test results showed that damage in the beam cover concrete and out-of plane deformation in the thinner slab reduced the gap-open in the post-tensioned frame, resulting in less efficiency of the force transfer in the slab.

The first intention of this paper is to propose a remedial detail of the floor slab as shown in Cheng and Ke 2007 that not only have the self-centering function but also can transfer the seismic loads. The second intention of this paper is to investigate the seismic performance of the self-centering structure under biaxial loads that may force the gap to open in two directions. To validate, a one-story 3D precast/post-tensioned reinforced concrete sub-structure was constructed and tested. The specimen design and test results are introduced in the followings.

2. THE SPECIMEN DESIGN

In order to investigate the force transfer of floor slabs between the gravity and moment-resisting frames, a one-span-one-story space frame with floor slab was constructed as shown in Fig. 1. The space frame spans at 6 and 5 meters center in the X and Y direction, respectively. There are four columns, four beams and one floor slab that compose two primary frames: gravity frame and moment-resisting frame (PT frame). The reinforced concrete columns 650x650x3200 mm in size seating on a bi-directional steel hinge were reinforced with 12D36 rebars longitudinally and D13 hoops spaced at 100 mm inside the panel zone and 150 mm outside the panel zone. The reinforced concrete beams are 500x600x5350 mm and 500x600x4350 mm in the X and Y direction, respectively. They were reinforced with 8D36 rebars longitudinally and D13 stirrups spaced at 100 mm. The beam and columns in the gravity frame were precast and then connected by a DSI6803 G270 strand post-tensioned to totally 233 kN representing 0.05Mn (5% of nominal strength of the beam=233x0.3=70 kN-m), while they are connected by 2-DSI 6808 G270 strands post-tensioned to totally 933 kN representing 0.20Mn for the moment-resisting frame. Two transfer beams between two frames were connected to the columns by 2-DSI6803 G270 strand and post-tensioned to totally 560 kN representing 0.10 Mn (560x0.25=140 kN-m) if it is required. To protect the cover concrete in the beam-column interface from crushing during the gap-open, the column and beam-end interfaces were all reinforced with 30 mm steel plates. In addition, all beam-ends were covered by a 20 mm thick 300 mm long steel band plate.

The floor consists of two hollow slabs, which are 4500x2500x300 mm in size with 150 mm diameter hole spaced at 278 mm inside the slab. Each slab was reinforced with 24-D22 rebars longitudinally and D13 stirrups spaced at 100 mm. 2-DSI 6807 strands was applied for each slab and post-tensioned to 197 kN representing 0.25 of nominal strength of the slab (197x1.25x2=492.5 kN-m). For protecting the cover concrete from crushing, a 15 mm thick 300 mm square steel cover plate was applied to reinforce each corner of the slab, in addition to the 15 mm thick 100 mm long steel band plate at the ends of the slabs adjacent to the beams. During the erection, the beams and slabs temperately positioned on the steel angles without bolts before being post-tensioned. In case of adding energy dissipating devices to the post-tensioned frame, steel angles L300x200x20 mm in size were installed at the top and bottom of the beam-ends with 7-25 mm A325 bolts, in which 3 fixed at the column face and 4 on the beam. Fig. 2 shows the image of the 3D structure after erection.

The material strengths of the concrete for the four components are 45 MPa on average on 28 days. The tested yield strength of Grade 60 rebars is close to 480MPa (70 ksi). The yielding and tensile strength of energy dissipating steel angles are 270 MPa and 417 MPa, respectively.

3. EXPERIMENTAL PROGRAM

Table 1 lists the investigated parameters including the applying prestress in each component, energy dissipating devices and loading compositions. Totally 3 groups of 9 tests were conducted. When the structure was loaded in the X direction only, the 1000 kN hydraulic actuator (X1) at top of the column in the gravity frame applied the cyclic loads with displacement control in the form of triangular waves, such as two cycles at 8mm (0.25%drift), 2mm (0.375%), 16mm (0.5%), 24mm (0.75%), 32mm (1.0%), 48mm (1.5%), 64mm (2%), 96mm (3%), and 128mm (4%). Then the loads were transmitted to the other column of the gravity frame by another 1000 kN actuator (X2), which applied the cyclic load with the load control set to be half amount of the actuator X1. All the lateral loads were then transmitted to the PT frame through the floor slab and transfer beams if it is prestressed. To ensure the movement of the gravity frame parallel to the loading direction, two 1000 kN actuators were mounted on the beam-end of the gravity frame, as shown in Fig. 3, with zero displacement control. When the structure was loaded in the Y direction only, the two actuators at the beam–end of the gravity frame applied the cyclic loads with displacement control in the form of triangular waves, such as two cycles at 8mm (0.25%drift), 2mm (0.375%), 16mm (0.5%), 24mm (0.75%), 32mm (1.0%), 48mm (1.5%), 64mm (2%), 96mm (3%), and 128mm (4%). The actuators in the X direction were free without loads.

When the structure was loaded in the bi-direction such as 4% in X and 2% in Y direction as shown in Fig. 4, the actuators in the X and Y directions independently applied the cyclic loads with displacement control in the form of triangular waves such as one cycle at 128mm (4%) and 64mm (2%) drift, respectively at the same time. During all loading protocols, the loading rate for all actuators was set to be 1mm/sec as static as possible. When the structure subjected to the uni-axial loads, the gap in the beam-slab interface may open and the slab stands up on the corners to form a line contact with the beam. However, when the structure subjected to the bi-axial loads, the gap may open in two directions. The original line contact in the interface may change to be a point contact, resulting in undesirable increase of sliding in the interface. To stop this sliding, the triangular steel shear keys were mounted on the gravity beam surface. In addition, to simulate the hinge behavior of the gravity frame, limited prestress was applied so that beam slips on the column face could be inevitable, therefore, steel shear keys at the top and bottom corners of the beam were vertically welded on the column face. To measure the gap-open in the interface of beams, slabs and columns, rotations of slabs and beams, and the movement of frames, many displacement transducers and clinometers were installed.

4. TEST RESULTS

The 3D structure was repeatedly tested 9 times without inducing any damage or plastic deformations. Under lateral loads, the structure behaved in an elastic manner with limited energy dissipation. The gaps in the slab, beam and column interface opened under loads and closed after loads sequentially. Fig. 5 illustrates the hysteretic loops and envelope of the force-deformation for the tests under X direction loading only. In these figures, the force superposes the lateral loads recorded in the two actuators at the top of columns, while the displacement represents the displacement control in the X1 actuator (at the top of C1 column as shown in Fig. 3). In the first few cycles of loading the gaps in the interfaces did not opened and the structure deformed according to its flexural stiffness. After 1.5% drift of loading, the gaps in the interfaces sequentially opened and the structure drifted with a constant stiffness. In the first two group tests the structure was designed to behave in an elastic manner with limited energy due to the friction force in the interfaces. In the third group test plastic deformations in steel angles occasionally contributed little energy dissipation. The strain gauges installed on the steel angles at one of the beam-ends yielded during 4% drift of loading. Comparison of the envelope of the force-deformation in three tests shows that the application of prestress in the transfer beams (test 2) and additional installation of the steel angels (test 3) slightly increased the lateral resistance of the structure loaded in the X direction only.

Fig 6 shows the displacement composition among the slab, PT frame and slips in the interfaces for the three tests under X direction of loading. The displacements Δ_{GF} in the figure were calculated by the superposition of displacements at the mid-height of the column (C1) and the displacements due to the gap-open in the beam-column (C1) interface of the gravity frame. This displacement represents the movement of the beam in the gravity frame under X direction of loading. The slips in the interfaces can be obtained from the total displacements Δ_{GF} subtracted the displacements recorded in the slab and PT frame. As shown in Fig. 6, the second test has the largest displacements in the PT frame but least amount of displacement in the slab and slips among three tests. In addition, Table 2 summarizes the interstory drift and gap-open in the slab and PT frame for the structure subjected to uni-axial or bi-axial loading. It can be seen that the second test also has the best efficiency in the force transfer with the largest drift and gap-open in the PT frame and the least in the slab. As shown in the Table, applying prestress in the transfer beams moved the PT frame 2.9% under 4% drift of loading in the gravity frame, compared with 2.0% without the prestress. However, adding the steel angles in the PT frame moved the PT frame only 2.3% under 4% drift of loading in the gravity frame, because of the stiffness increase in PT frame. Therefore, the level of post-tensioning force in the slab, transfer beams and PT frame significantly change their stiffness and then affect the efficiency of force transfer in the slab. The more the post-tensioning force in the slab and transfer beams and the less the post-tensioning loads in the PT frame are applied, the higher the slab stiffness is and the more the gap in the PT frame may be opened.

Fig. 7 illustrates the hysteretic loops and envelope of the force-deformation for the tests under Y direction loading only. The structure behaved in an elastic manner as in the tests loaded by the X direction only. For the structure loaded in Y direction only, the hysteretic energy contributed from the friction force in the interfaces. As shown in the force-deformation envelope, applying prestress in the transfer beams (test 2) largely increased the lateral resistance of the structure in the Y direction. However, adding steel angles (test 3) had only marginal effect on the lateral resistance of the structure. Fig. 8 shows the force-deformation relations of the structure subjected to uni-axial or bi-axial loading respectively. It can be seen that the lateral resistance of the structure subjected to bi-axial loading is slightly less than the one under uni-axial loading. This may be attributed to the increase of sliding in the point-contact interface of the slab and beams, when the structure subjected to a bi-axial loading. This can also be seen from Table 2 where the drift and opening in the slab increased along with a slightly decrease of the drift and opening in the PT frame for the structure subjected to a bi-axial loading. This indicates that bi-axial loads open the gap of the slab-beam interfaces in two directions, reduce the slab stiffness and then indirectly decrease the efficiency of the force transfer in the slab, but not by a substantial margin due to the relatively small thick/length ratio of the slab (0.3/2.5 in this test).

5. CONCLUSIONS

Based on the experimental investigation of a self-centering designed 3D structure, it was found that the structure, sequentially tested 9 times under uni-axial or bi-axial loads, behaved in an elastic manner without any damage and plastic deformations. Limited hysteretic energy of the structure contributed by the friction force in the interfaces was observed for all tests. The lateral resistance of the structure was significantly increased in the parallel direction (Y), but only slightly increased in the orthogonal direction (X) due to the application of prestress to the transfer beams. Adding steel angels to the PT frame slightly reduced the efficiency of the force transfer in the X direction loading but had only marginal effect in the Y direction loading. The level of post-tensioning force in the slab, transfer beams and PT frame significantly affect the efficiency of force transfer in the slab. The more the post-tensioning force in the slab and transfer beams and the less the post-tensioning loads in the PT frame are applied, the more the slab transmits the seismic load. Under bi-axial loads, slab-beam interfaces opened in two directions that increased the sliding and reduced the efficiency of the force transfer by the slab, but not by a substantial margin due to the relatively small thick/length ratio of the slab.

ACKNOWLEDGEMENTS

The research reported herein has been conducted as part of the result of a series of research projects granted by

the Taiwan Science Council to the author with NSC95-2625-Z-327-003.

REFERENCES

Cheng, C.-T., and Ke, W.-L.(2007). The Force Transfer of Floor Slabs in a 3D Precast/Post-tensioned Reinforced Concrete Sub-structure. Paper No. 063, The 8th Pacific Conference on Earthquake Engineering (8PCEE), December 5-7, 2007, Singapore.

Christopoulos, C., Filiatraut, F., Uang, C.M. and Folz, B. (2002). Post-tensioned energy dissipating connections for moment resisting steel frames. *Journal of Structural Engineering, ASCE*, 128 (9), 1111-1120.

Garlock, M. and Li, J. (2005). Floor diaphragm interaction with self-centering steel moment resisting frames. US-Taiwan Workshop on Self-centering Structural Systems, June 6-7, 2005, Taipei, Chinese Taiwan, edited by K.C. Tsai and Ricles, J. NCREE report No. 05-004, 34-35.

Ricles, J.M., Sauce, R., Peng, S.W. and Lu, L.W. (2002). Experimental evaluation of earthquake resistant post-tensioned steel connections. *Journal of Structural Engineering, ASCE*, 128 (7), 850-859.

Table 1 Investigated parameters

Tests	Prestress		E.D. Angles	Loading Compositions	
	Floor	T. Beam		X	Y
1	25%	N	N	4%	N
				N	4%
				4%	2%
2	25%	10%	N	4%	N
				N	4%
				4%	2%
3	25%	10%	Y	4%	N
				N	4%
				4%	2%

Table 2 Drift and gap-open in the slab and PT frame under X-4% drift of loading

PT frame	Uni-axial (%)		Bi-axial (%)	
	Drift	Gap-open	Drift	Gap-open
1	1.98	2.26	1.85	2.09
2	2.89	3.24	2.61	2.90
3	2.27	2.55	1.75	1.94
Slab	**Uni-axial (%)**		**Bi-axial (%)**	
	Drift	Gap-open	Drift	Gap-open
1	1.03	0.50	1.08	0.52
2	0.57	0.27	0.62	0.29
3	1.05	0.50	1.04	0.49

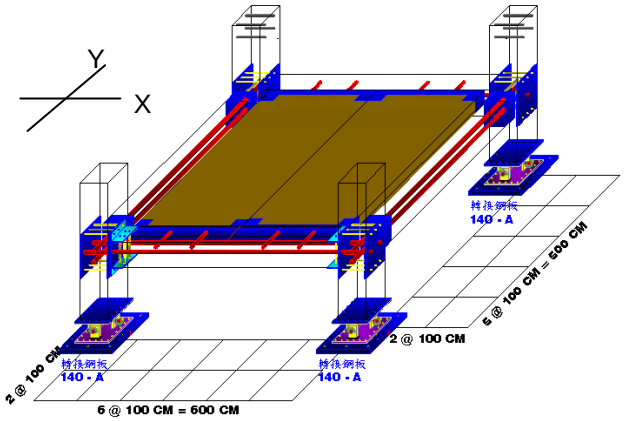

Fig. 1 Tested 3D specimen

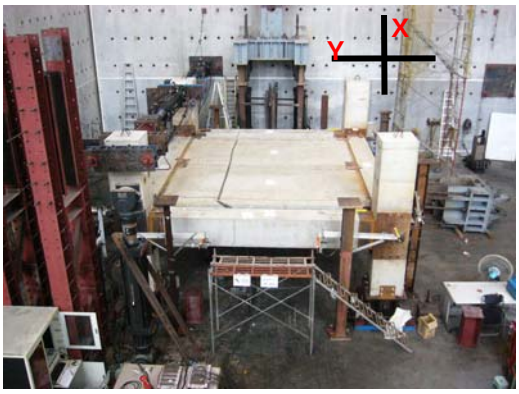

Fig. 2 Photo showing the specimen after erection

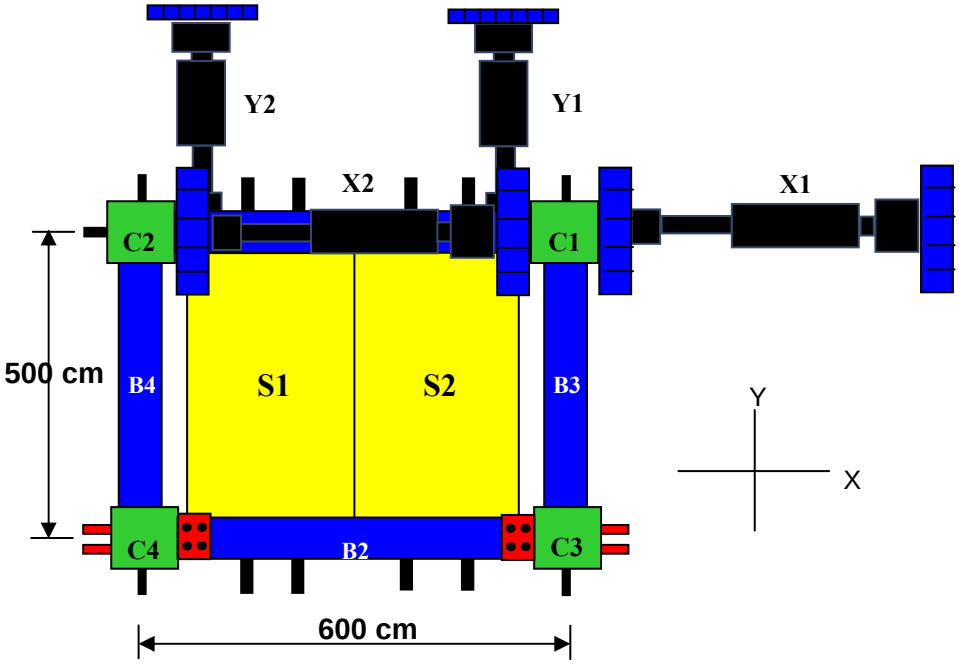

Fig. 3 Test setup

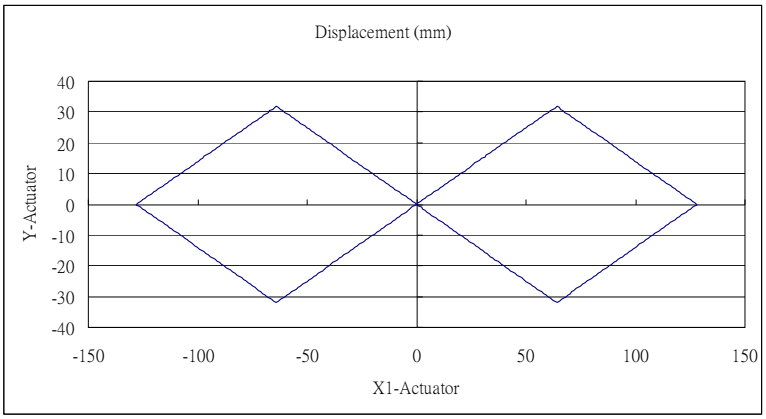

Fig. 4 Relations of two orthogonal displacements in the bi-axial tests

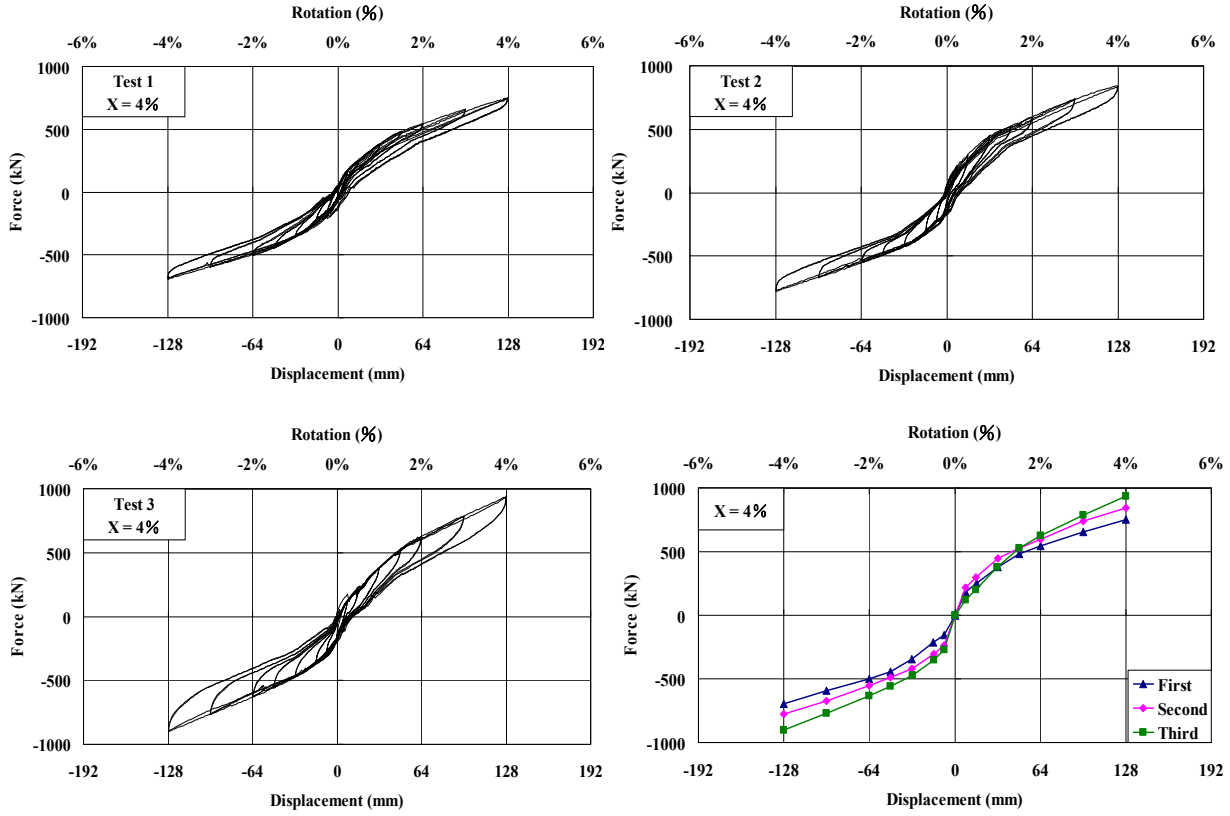

Fig. 5 Hysteretic loops and envelope under X direction loading

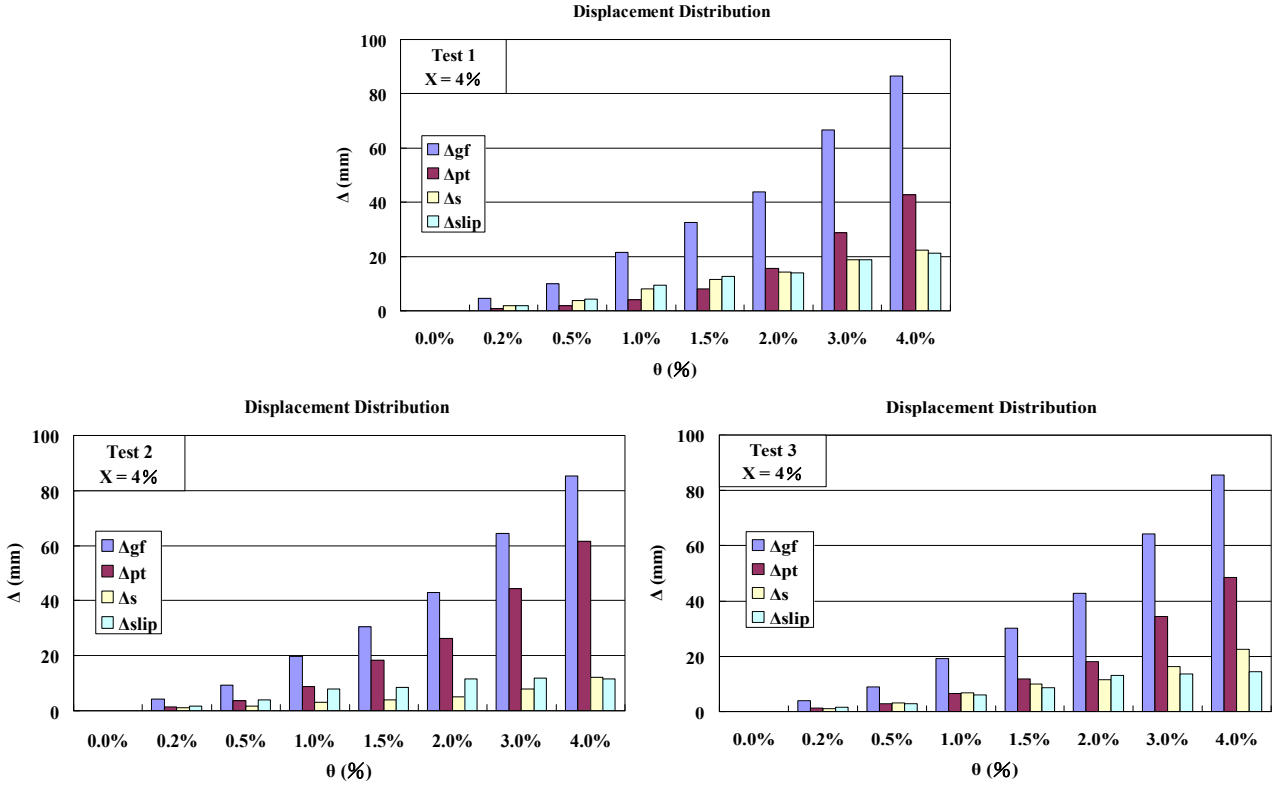

Fig. 6 Displacement composition in the structure under X direction loading

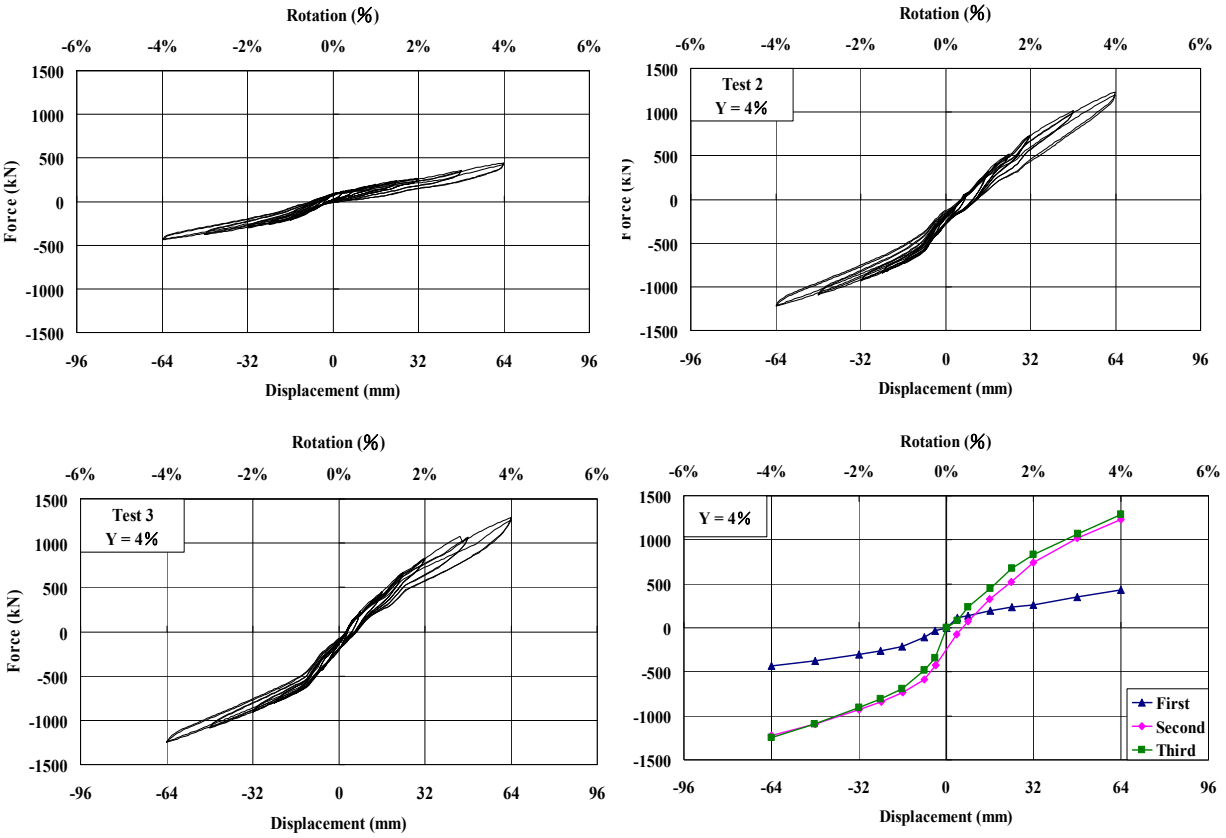

Fig. 7 Hyteretic loops and envelope under Y direction loading

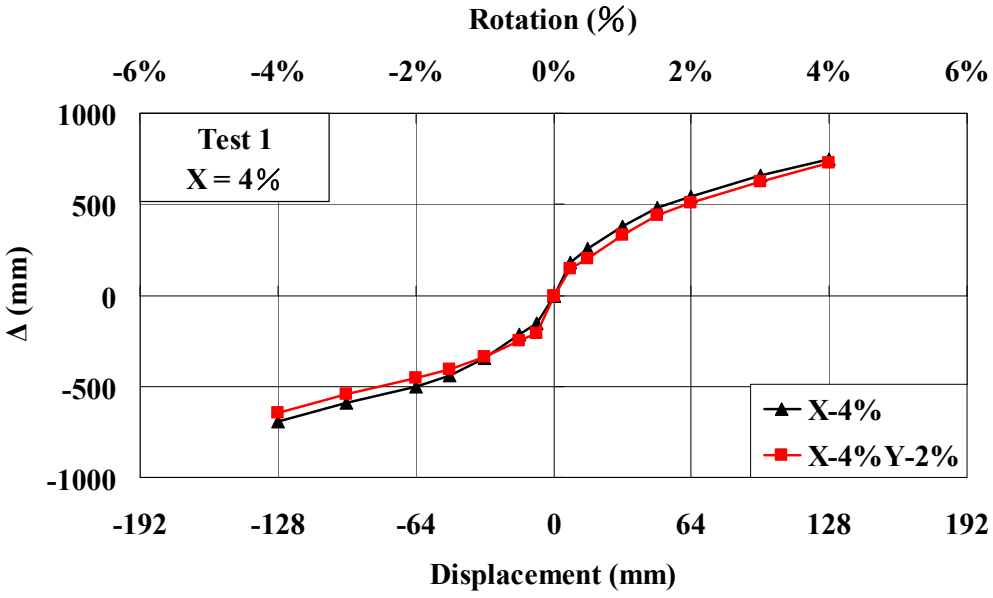

Fig. 8 Force-deformation envelope for the tests under uni-axial or bi-axial loads